Vol. 39 (2008) ACTA PHYSICA POLONICA B No 12

TOPICS IN CUSPED/LIGHTCONE WILSON LOOPS*

Yuri Makeenko†

Institute of Theoretical and Experimental Physics
117218 Moscow, Russia
makeenko@itep.ru

(Received October 20, 2008)

I review several old/new approaches to the string/gauge correspondence for the cusped/lightcone Wilson loops. The main attention is payed to SYM perturbation theory calculations at two loops and beyond and to the cusped loop equation.

PACS numbers: 11.15.Pg, 11.25.Tq, 11.30.Pb

The paper is organized as follows. In Sect. 1 a pedagogical introduction is given, including Wilson loops with cusps and their renormalization, their relation to twist-two operators and the role they play in string/gauge correspondence. Finally I discuss minimal surface in $\mathrm{AdS}_5 \otimes S^5$ for cusped loops. Sect. 2 is devoted to perturbation theory to two loops and beyond. In this context I discuss exact sum of ladders, explicit two loop calculation and the anomaly terms. I also summarize results in the double logarithmic approximation and describe problems with planar QFT. Finally in Sect. 3 I discuss cusped loop equation. First I present modern formulation of the loop equation, then I introduce SUSY extension and discuss UV regularization and specifics of cusped loops. I close by computing cusp anomalous dimension from the loop equation.

For completeness of this paper I added three appendices with some detail not given in the lectures but which might be useful for the reader.

---

* Presented at the XLVIII Cracow School of Theoretical Physics, “Aspects of Duality”, Zakopane, Poland, June 13–22, 2008.

† Also at the Institute for Advanced Cycling, Blegdamsvej 19, 2100 Copenhagen Ø, Denmark.

1. Pedagogical introduction

I review in this section Wilson loops with cusps, their renormalization and the relation to twist-two operators. Then I discuss the role played by the cusped Wilson loops in the string/gauge correspondence and describe a proper minimal surface in $\mathrm{AdS}_5 \otimes S^5$ associated with cusped loops.

1.1. Wilson loops

Wilson loops play a crucial role in modern formulations of gauge theories since the work by Wilson (1975).

The construction is based on a non-Abelian phase factor

$$U(C) = \boldsymbol{P} e^{ig \int_C A_\mu(x) dx^\mu} \stackrel{\text{def}}{=} \prod_{x \in C} (1 + igA_\mu(x) dx^\mu) \tag{1.1}$$

which is nothing but a parallel transporter in an external non-Abelian Yang–Mills field $A_\mu(x)$. The trace over matrix indices $\operatorname{Tr} U(C)$ is gauge-invariant for closed C.

The Wilson loop vacuum expectation value (or the average in Euclidean formulation) is defined by

$$W(C) = Z^{-1} \int \mathcal{D}A_\mu \, \mathcal{D}\bar{\psi}\mathcal{D}\psi \cdots e^{iS} \frac{1}{N} \operatorname{Tr} U(C) \,, \tag{1.2}$$

where the path integration goes over Yang–Mills and quark fields.

The importance of the Wilson loops in QCD is because

- observables are expressed via sum-over-path of $W(C)$,
- dynamics is entirely reformulated via $W(C)$.

These statements hold strictly speaking only at large N, while at finite N correlators of several Wilson loops appear which factorize in the large-N limit. Wilson loops $W(C)$ obey the loop equation which is a closed equation on loop space at large N (see the book by Makeenko (2002) for more detail on these issues).

It is important that typical loops which are essential in the sum-over-path are *cusped.* The properties of the Wilson loops of this kind differ from those for smooth loops, *e.g.* a circular loop.

1.2. Renormalization of smooth Wilson loops

Renormalization properties of *smooth* Wilson loops are studied by Gervais, Neveu (1980), Polyakov (1980), Vergeles, Dotsenko (1980). They become finite after the charge renormalization:

$$W(g;C) = e^{-\text{const.}\,L(C)/a}\,W_{\rm R}(g_{\rm R};C)\,, \tag{1.3}$$

where $W_{\rm R}$ is finite after the charge renormalization $g \Longrightarrow g_{\rm R}$ and a is a certain (gauge-invariant) UV cutoff.

The exponential perimeter factor in Eq. (1.3) is associated with the renormalization of the mass of a heavy test particle propagating along the loop. It does not emerge in dimensional regularization.

1.3. Renormalization of cusped Wilson loops

An additional logarithmic divergence appears for cusped loops as was first discovered by Polyakov (1980). A cusped Wilson loop is depicted in Fig. 1.

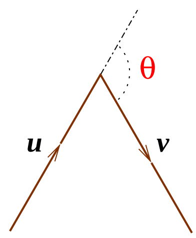

Fig. 1. Segment of a closed loop near the cusp. The cusp angle θ is formed by the vectors u and v: $\cosh\theta = \frac{u\cdot v}{\sqrt{u^2}\sqrt{v^2}}$.

The cusped Wilson loops are multiplicatively renormalizable as was shown by Brandt, Neri, Sato (1981):

$$W(g;\Gamma) = Z(g;\theta) W_{\rm R}(g_{\rm R};\Gamma)\,, \tag{1.4}$$

where (the divergent factor of) $Z(g;\theta)$ depends on the cusp angle θ.

Equation (1.4) is true only when the contour Γ has no light-cone segments. The peculiarities of the renormalization of light-cone Wilson loops are described below.

1.4. Cusp anomalous dimension

The cusp anomalous dimension is defined by the formula

$$\gamma_{\rm cusp}\,(g;\theta) = -a\frac{d}{da}\ln Z(g;\theta)\,, \tag{1.5}$$

where Z is the renormalizing factor in Eq. (1.4).

The cusp anomalous dimension depends in general both on the coupling constant g and on the cusp angle θ. A very important observation by Korchemsky, Radyushkin (1987) is that in the limit of large θ it is linear in θ:

$$\gamma_{\rm cusp}\,(g;\theta) \stackrel{\theta\to\infty}{\to} \frac{\theta}{2} f(g)\,. \tag{1.6}$$

The same function $f(g)$ appears in the anomalous dimensions of twist-two conformal operators with large spin.

1.5. Conformal operators of twist two

Anomalous dimensions of twist-two operators of the type

$$O_J^{(F)} = \frac{1}{N}\,{\rm Tr}\,F_{\mu\cdot}\,(\nabla .)^{J-2}\,F_{\mu\cdot}\,, \tag{1.7}$$

$$O_J^{(\Psi)} = \bar{\Psi}\gamma.\,(\nabla .)^{J-1}\,\Psi \tag{1.8}$$

with Lorentz spin J are measurable in deep inelastic scattering. The operators in Eq. (1.7) are constructed from gauge field and those in Eq. (1.8) are constructed from quarks.

In $\mathcal{N} = 4$ supersymmetric Yang–Mills (SYM) there are also analogous operators

$$O_J^{(\Phi)} = \frac{1}{N}\,{\rm Tr}\,\Phi\,(\nabla .)^J\,\Phi \tag{1.9}$$

constructed from scalars.

The following notation is used in Eqs. (1.7), (1.8) and (1.9):

$$\nabla . \equiv \nabla_\mu \xi_\mu \qquad \xi^2 = 0\,. \tag{1.10}$$

This multiplication by a light-like vector ξ provides symmetrization and subtraction of traces, as is needed for a representation of the Lorentz group.

What is depicted in Eqs. (1.7), (1.8) and (1.9) by $(\nabla .)^J$ is in fact a polynomial in $\overleftarrow{\nabla}.$ and $\overrightarrow{\nabla}.$, the covariant derivatives acting on the left and on the right. At the one-loop level it is a Gegenbauer polynomial dictated by conformal invariance as was shown by Brodsky, Frishman, Lepage, Sachrajda (1980), Makeenko (1981), Ohrndorf (1982). These conformal operators are multiplicatively renormalizable at one loop and form a convenient basis for two-loop computations.

1.6. Relation between the anomalous dimensions

The relation between twist-two operators and cusped Wilson loops can be understood by considering an open Wilson loop with matter fields attached at the ends:

$$O(C_{y0}) = \bar{\psi}(y)\boldsymbol{P}e^{\mathrm{i}g\int_0^y d\xi^\mu A_\mu}\psi(0)\,. \tag{1.11}$$

The case when this open loop is a straight line from 0 to y is depicted in Fig. 2.

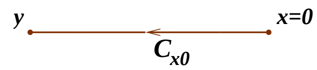

Fig. 2. Straight Wilson loop from 0 to y.

The standard triangular diagrams, which give the anomalous dimension like in Gross, Wilczek (1973), come from the formula

$$\left\langle \psi(\infty,\vec{y})O(C_{y0})\bar{\psi}(\infty,\vec{0})\right\rangle \propto W(\Pi) \tag{1.12}$$

as mass of matter fields $\to\infty$. The Wilson loop which emerges on the right-hand side is Π-shaped as is depicted in Fig. 3. The vertical lines represent propagation (in time) of static quarks, sitting at $\vec{0}$ and $\vec{y}$, which are connected by the straight line associated with the open Wilson loop.

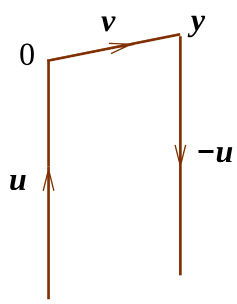

Fig. 3. Π-shaped Wilson loop.

To derive Eq. (1.12), remember that the propagator in an external field A_μ is

$$\left\langle \psi_i(x)\bar{\psi}_j(y)\right\rangle_\psi \overset{\text{large } N}{=} \sum_{C_{yx}} \left[e^{\mathrm{i}g\int_{C_{yx}} d\xi^\mu A_\mu}\right]_{ij} \overset{\text{mass}\to\infty}{\propto} \left[e^{\mathrm{i}g\int_{C_{yx}^{(\min)}} d\xi^\mu A_\mu}\right]_{ij} \tag{1.13}$$

and thus the straight vertical lines appear in Π.

The central segment of Π is near the light-cone to suppress the contribution from operators of twists higher than two. Π has two cusps with $\theta \to \infty$.

This is how the light-cone Wilson loop is related to the conformal operators of twist two.

1.7. Light-cone Wilson loops

For the Π-shaped loop with 1 light-cone segment as in Fig. 3, we have

$$W(\Pi) = e^{-\frac{1}{2}f(\lambda)\ln^2\frac{T}{a}+\mathrm{const.}(\lambda)\ln\frac{T}{a}+\mathrm{finite}(\lambda)} \tag{1.14}$$

with the same $f(\lambda)$ as before, as was shown by Korchemsky, Marchesini (1993). Here v^μ is along the light cone ($v^2 = 0$) and $y_\mu = v_\mu T$.

A very closely related (and more simple!) object, proposed by Alday, Maldacena (2007), is a Γ-shaped loop which is formed by 2 light-cone segments:

$$W(\Gamma) = e^{-\frac{1}{2}f(\lambda)\ln\frac{T}{a}\ln\frac{S}{a}+g(\lambda)(\ln\frac{T}{a}+\ln\frac{S}{a})+\mathrm{finite1}(\lambda)}\,. \tag{1.15}$$

Now both v^μ and u^μ are along the light cones ($v^2 = 0$, $u^2 = 0$) and $y_\mu = v_\mu T$, $x_\mu = u_\mu S$. Most probably it gives the same $f(\lambda)$ but this is not yet rigorously proved.

1.8. SYM Wilson loops

An extension of Wilson loops to $\mathcal{N} = 4$ supersymmetric Yang–Mills (SYM) was given by Maldacena (1998):

$$W_{\mathrm{SYM}}(C) = \left\langle \frac{1}{N}\,\mathrm{Tr}\,\boldsymbol{P}e^{\mathrm{i}g\oint_C d\sigma\left(\dot{\xi}^\mu A_\mu + |\dot{\xi}|n^i\Phi_i\right)}\right\rangle \tag{1.16}$$

with unit vector $n^i \in S^5$ ($n^2 = 1$) and 6 scalars Φ_i ($i = 1,\cdots,6$). In Minkowski space there is no relative i between the two terms in the exponent in Eq. (1.16), which is present in Euclidean space.

Under a supersymmetry transformation

$$\delta A_\mu = \bar{\Psi}\Gamma_\mu\zeta\,, \qquad \delta\Phi_i = \bar{\Psi}\Gamma_i\zeta\,, \tag{1.17}$$

where an infinitesimal parameter ζ is a 10d Majorana–Weyl spinor and (Γ_μ, Γ_i) are 10d gamma matrices, the SYM Wilson loop (1.16) remains unchanged if

$$\left(\Gamma_\mu\dot{\xi}^\mu + \Gamma_i|\dot{\xi}|n^i\right)\zeta = 0\,. \tag{1.18}$$

Noting that the combination of gamma matrices in the brackets is nilpotent for timelike $\dot{\xi}$, Eq. (1.18) is satisfied when a half components of ζ vanish.

An example of such a BPS state possessing a half of supersymmetries is the SYM Wilson loop for a straight line inside the light-cone, for which we have

$$W_{\mathrm{SYM}}(|) = 1\,. \tag{1.19}$$

An adjoint Wilson loop is related to the fundamental-representation one by the formula

$$\mathrm{Tr}_A\, U = |\,\mathrm{Tr}\, U|^2 - 1\,. \tag{1.20}$$

Due to factorization at large N we have

$$\left\langle \frac{1}{N^2}\,\mathrm{Tr}_A\, U(C) \right\rangle = \left\langle \frac{1}{N}\,\mathrm{Tr}\, U(C) \right\rangle^2\,, \tag{1.21}$$

where the adjoint Wilson loop is on the left-hand side and the (square of the) fundamental one is on the right-hand side.

The same results as mentioned above for QCD hold for SYM Wilson loops and there are some more. In particular, the perimeter factor in Eq. (1.3) is missing for SYM Wilson loops owing to the cancellation between gauge fields and scalars.

1.9. Motivation (since 2002)

A remarkable prediction for the anomalous dimension of twist-two operators with large (Lorentz) spin J, based on the AdS/CFT correspondence, was made by Gubser, Klebanov, Polyakov (2002). It states that

$$\varDelta - J - 2 = f(\lambda)\ln J\,, \qquad \text{large } J \tag{1.22}$$

with

$$f(\lambda) = \frac{\sqrt{\lambda}}{\pi}\,, \qquad \text{large } \lambda = g^2_{\mathrm{YM}} N\,. \tag{1.23}$$

It stems from the spectrum of closed folded string which is rotating in AdS_5.

The same result holds for the cusp anomalous dimension at large θ in the supergravity approximation to the AdS/CFT correspondence as is demonstrated by Kruczenski (2002), Makeenko (2003) and reviewed by Alday, Roiban (2008). For completeness of this paper I describe the proper minimal surface in $\mathrm{AdS}_5 \otimes S^5$ in Appendix A.

Equations (1.22), (1.23) have been remarkable reproduced recently from the spin chain S-matrix by Staudacher (2005), Eden, Staudacher (2006), Beisert, Eden, Staudacher (2007). Many more results are obtained along this line as is reviewed in the lectures by M. Staudacher at this School.

Remarkably, the same function $f(\lambda)$ appears in MHV gluon amplitudes for SYM as conjectured by Bern, Dixon, Smirnov (2005) on the basis of a few lower orders of SYM perturbation theory and further elaborated by Bern, Czakon, Dixon, Kosower, Smirnov (2007). This subject is reviewed in the Alday, Roiban (2008) The BDS amplitude is reproduced for large λ from the AdS/CFT correspondence by Alday, Maldacena (2007) and is reviewed in the Alday, Roiban (2008).

It is a challenging problem to obtain $\sqrt{\lambda}$ for the cusp anomalous dimension at large λ in SYM perturbation theory. I shall describe some steps along this line in Sects. 2 and 3.

1.10. AdS/CFT for Wilson loops

The formulation of the AdS/CFT correspondence between Wilson loops and open IIB strings in the $\mathrm{AdS}_5 \otimes S^5$ background was given by Maldacena (1998), Rey, Yee (1998). The statement is that the SYM Wilson loop equals the sum over open surfaces bounded by the contour C:

$$W_{\mathrm{SYM}}(C) = \sum_{S:\partial S = C} e^{\mathrm{i}A_{\mathrm{IIB\ on\ AdS_5 \otimes S^5}}} \,. \tag{1.24}$$

Here

$$C = \left(x^\mu(\sigma), \int^{\sigma} d\sigma \, |\dot{x}(\sigma)| n^i(\sigma) \right) \tag{1.25}$$

is a (9-dimensional loop) in the boundary of $\mathrm{AdS}_5 \otimes S^5$, *e.g.* for $n^i = (1,0,0,0,0,0)$ only a 4d contour $x^\mu(\sigma)$ remains. Equation (1.24) is graphically represented in Fig. 4.

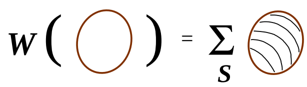

Fig. 4. Open-string/Wilson-loop correspondence.

For a circular loop there is a remarkable perfect agreement between the AdS supergravity calculation by Berenstein, Corrado, Fischler, Maldacena (1998), Drukker, Gross, Ooguri (1999) and the CFT SYM calculation by Erickson, Semenoff, Zarembo (2000), Drukker, Gross (2001).

However, the situation is not as good for a rectangular loop (or antiparallel lines), when the minimal surface in $\mathrm{AdS}_5 \otimes S^5$ was found by Maldacena (1998), Rey, Yee (1998), and the summation of ladder diagrams of the type depicted in Fig. 5 was performed by Erickson, Semenoff, Szabo, Zarembo (1999), Erickson, Semenoff, Zarembo (2000).

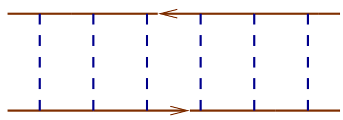

Fig. 5. Ladder diagrams for a rectangular Wilson loop.

The results are:

AdS: SYM:

$$V(R) = -\frac{4\pi^2\sqrt{2\lambda}}{\Gamma^4(1/4)R}\,, \qquad V(R) = -\frac{\sqrt{\lambda}}{\pi R}\,. \tag{1.26}$$

The coefficients in these two results obviously do not agree. The discrepancy is customary attributed to interaction diagrams... But a remark is that the SYM coefficient is what is needed for the cusp anomalous dimension at large λ.

2. Perturbation theory: two loops and beyond

In this section I describe how to sum up ladder diagrams of perturbation theory and explicitly consider the two-loop order where a cancellation of interaction diagrams is not complete resulting in an anomaly term. I analyze light-cone Wilson loops in the double logarithmic approximation which gives a hint on higher-order anomaly terms and reveals problems with planar QFT in describing the results.

2.1. One-loop perturbation theory

Diagrams of perturbation theory for SYM Wilson loops can be constructed by expanding Eq. (1.16) in the coupling constant λ.

To the order λ (one-loop order) we have explicitly

$$W(\Gamma) = 1-\frac{\lambda}{2}\int\limits_{-\infty}^{+\infty} d\sigma_1 \int\limits_{-\infty}^{+\infty} d\sigma_2 \Big[\dot{x}^\mu(\sigma_1)\dot{x}_\mu(\sigma_2)-|\dot{x}(\sigma_1)||\dot{x}(\sigma_2)|\Big] D\left(x(\sigma_1)-x(\sigma_2)\right), \tag{2.1}$$

where

$$D(x) = -\frac{\Gamma\left(d/2-1\right)}{4\pi^{d/2}}\left[-x^2\right]^{1-d/2} \tag{2.2}$$

is the (scalar) propagator in d-dimensions.

The double integral on the right-hand side of Eq. (2.1) can be represented as the sum of three diagrams in Fig. 6, where dashed lines correspond to either gluon or scalar propagators. Actually, the diagrams (a) and (c) vanish because gluons are cancelled by scalars (like in Eq. (1.19)).

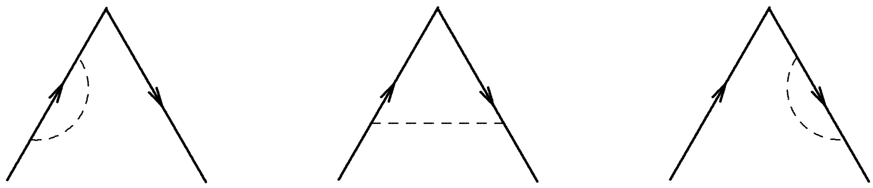

(a) (b) (c)

Fig. 6. Diagrams of perturbation theory to order λ. Diagrams (a) and (c) vanish (gluons are canceled by scalars).

For the only nonvanishing diagram in Fig. 6(b), we have

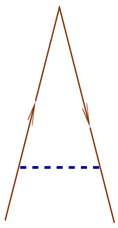

$$
\begin{aligned}
W(\Gamma) &= 1-\frac{\lambda}{4\pi^2}(\cosh\theta-1)\int ds\int dt\,\frac{1}{s^2+2st\cosh\theta+t^2}\\
&= 1-\frac{\lambda}{4\pi^2}\frac{\cosh\theta-1}{\sinh\theta}\theta\ln\frac{L}{a}\\
&\overset{\text{large }\theta}{\to} 1-\frac{\lambda}{4\pi^2}\theta\ln\frac{L}{a}
\end{aligned}
\tag{2.3}
$$

$$
\text{which yields} \qquad \Longrightarrow \qquad f(\lambda)=\frac{\lambda}{2\pi^2}\,. \tag{2.4}
$$

Notice that, in contrast to QCD, in SYM there is no mass-renormalization term $-\lambda/4\pi a$.

An exact formula for the order λ result is

$$
\begin{aligned}
W(S,T;a,b) &= 1-\frac{\lambda}{4\pi^2}(\cosh\theta-1)\int_a^S ds\int_b^T dt\,\frac{1}{s^2+2st\cosh\theta+t^2}\\
&= 1-\frac{\lambda}{8\pi^2}\frac{\cosh\theta-1}{\sinh\theta}\left(\mathrm{Li}_2\left(-\frac{T}{S}e^{\theta}\right)-\mathrm{Li}_2\left(-\frac{T}{S}e^{-\theta}\right)\right.\\
&\quad -\mathrm{Li}_2\left(-\frac{T}{a}e^{\theta}\right)+\mathrm{Li}_2\left(-\frac{T}{a}e^{-\theta}\right)-\mathrm{Li}_2\left(-\frac{b}{S}e^{\theta}\right)\\
&\quad \left.+\mathrm{Li}_2\left(-\frac{b}{S}e^{-\theta}\right)+\mathrm{Li}_2\left(-\frac{b}{a}e^{\theta}\right)-\mathrm{Li}_2\left(-\frac{b}{a}e^{-\theta}\right)\right)\,,
\end{aligned}
\tag{2.5}
$$

where we cut the integrals by S, T from above and by a, b from below.

In Eq. (2.5) Li_2 is Euler's dilogarithm

$$
\mathrm{Li}_2(z)=\sum_{n=1}^{\infty}\frac{z^n}{n^2}=-\int_0^z\frac{dx}{x}\,\ln(1-x) \tag{2.6}
$$

which obeys the relation

$$\mathrm{Li}_2\left(-e^{\Omega}\right)+\mathrm{Li}_2\left(-e^{-\Omega}\right)=-\frac{1}{2}\ln^2\Omega-\frac{\pi^2}{6}\,. \tag{2.7}$$

It is used to extract the double logarithms.

2.2. Double-logarithmic approximation

The final result for large θ in Eq. (2.3) can be extracted without an exact computation using a double logarithmic approximation (DLA) quite similar to the one for Sudakov's form-factor.

The one-loop integral

$$W(S,T;a,b)=1-2\beta(\cosh\theta-1)\int\limits_a^S ds\int\limits_b^T dt\,\frac{1}{s^2+2st\cosh\theta+t^2}\,, \tag{2.8}$$

where we have introduced

$$\beta=\frac{\lambda}{8\pi^2}\,, \tag{2.9}$$

has a *double-logarithmic* region of integration:

$$te^{-\theta}\lesssim s\lesssim te^{\theta} \qquad \text{or} \qquad se^{-\theta}\lesssim t\lesssim se^{\theta}\,. \tag{2.10}$$

As a consequence of this fact, we write Eq. (2.8) for $\theta\gg 1$ in DLA as

$$W(S,T;a,b)\stackrel{\text{DLA}}{=}1-\beta\int\limits_b^T\frac{dt}{t}\int\limits_{\max\{a,te^{-\theta}\}}^{\min\{S,te^{\theta}\}}\frac{ds}{s}\,. \tag{2.11}$$

Several limits are now possible. Let

$$1\ll\theta\lesssim\ln\frac{T}{b}\ll\ln\frac{S}{a}\,. \tag{2.12}$$

Then

$$W(S,T;a,b)\Longrightarrow 1-2\beta\theta\ln\frac{T}{b} \tag{2.13}$$

reproducing the above result (2.3).

Alternatively, if

$$\theta\gg\ln\frac{T}{b},\ \ln\frac{S}{a}\,, \tag{2.14}$$

we obtain

$$W(S,T;a,b)\Longrightarrow 1-\beta\ln\frac{T}{b}\ln\frac{S}{a} \qquad \boxed{\text{very large }\theta} \tag{2.15}$$

reproducing the result for 2 light-cone segments.

Some more results on the double logarithms are described in Appendix B.

2.3. Sum of ladder diagrams

As was explained in the Section 1, we are motivated to consider ladder diagrams of the type depicted in Fig. 7, which is a simplest class of diagrams of planar QFT.

The ladder diagrams can be summed using a Bethe–Salpeter equation

$$\mathcal{G}(S,T) = 1 - \frac{\lambda(\cosh\theta - 1)}{4\pi^2} \int_a^S ds \int_b^T dt \frac{\mathcal{G}(s,t)}{s^2 + 2st\cosh\theta + t^2} . \tag{2.16}$$

Several light-cone limits are again possible:
1 light-cone limit: $\theta \to \infty$ with fixed $T_{\rm l.c.} = 2Te^{\theta}$ resulting in

$$\mathcal{G}\,(S,T;a,b) = 1 - \beta \int_a^S ds \int_b^T dt\, \frac{\mathcal{G}\,(s,t;a,b)}{\alpha s^2 + st} , \tag{2.17}$$

where

$$\alpha = \frac{u^2}{2u \cdot v} \tag{2.18}$$

and β is given by Eq. (2.9) (remember that $v^2 = 0$ for the light-cone direction).
2 light-cone limit: for $\alpha = 0$ when additionally $u^2 = 0$, the cusped loop has 2 light-cone segments.

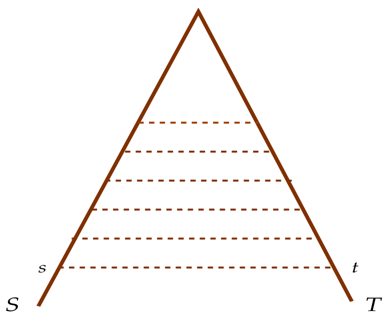

Fig. 7. Typical ladder diagram for a cusped Wilson loop.

2.4. The ladder equation

Differentiating Eq. (2.17) we obtain

$$S\frac{\partial}{\partial S}\,T\frac{\partial}{\partial T}\,\mathcal{G}\,(S,T;a,b) = -\frac{\beta}{1 + \alpha S/T}\,\mathcal{G}\,(S,T;a,b) \tag{2.19}$$

and analogously

$$a\frac{\partial}{\partial a}\, b\frac{\partial}{\partial b}\, \mathcal{G}\,(S,T;a,b) = -\frac{\beta}{1+\alpha a/b}\; \mathcal{G}\,(S,T;a,b) \tag{2.20}$$

with the boundary conditions

$$\mathcal{G}(a,T;a,b) = \mathcal{G}(S,b;a,b) = 1\,. \tag{2.21}$$

To separate variables, it is convenient to introduce the new variables

$$X = \ln\frac{S}{a} - \ln\frac{T}{b}\,, \qquad Y = \ln\frac{S}{a} + \ln\frac{T}{b}\,. \tag{2.22}$$

Then Eqs. (2.19) and (2.20) can be rewritten as

$$\left(\frac{\partial^2}{\partial X^2} - \frac{\partial^2}{\partial Y^2}\right)\mathcal{G} = \frac{\beta}{1+\alpha\frac{a}{b}e^X}\,\mathcal{G} \;\overset{\alpha S \ll T}{=}\; \beta\,\mathcal{G}\,. \tag{2.23}$$

It is similar to the equation by Erickson, Semenoff, Szabo, Zarembo (1999) but with different boundary conditions.

2.5. *Exact solution for ladders* ($\alpha = 0$)

A solution to Eq. (2.23) for $\alpha = 0$ is the Bessel function

$$\mathcal{G}_{\alpha=0}\,(S,T;a,b) = J_0\left(2\sqrt{\beta\ln\frac{S}{a}\ln\frac{T}{b}}\right) \tag{2.24}$$

which obviously obeys the boundary condition (2.21).

This can be easily shown by an iterative solution of

$$\mathcal{G}_{\alpha=0}\,(S,T;a,b) = 1 - \beta\int_a^S \frac{ds}{s}\int_b^T \frac{dt}{t}\,\mathcal{G}_{\alpha=0}\,(s,t;a,b)\,, \tag{2.25}$$

where the integrals over s and t decouple and both are logarithmic:

$$\mathcal{G}_{\alpha=0}\,(S,T;a,b) = \sum_{n=0}^{\infty}(-\beta)^n\frac{\left(\ln\frac{S}{a}\right)^n}{n!}\frac{\left(\ln\frac{T}{b}\right)^n}{n!} = J_0\left(2\sqrt{\beta\ln\frac{S}{a}\ln\frac{T}{b}}\right). \tag{2.26}$$

Asymptotically we have

$$J_k(z) \sim \cos z\,, \qquad \text{large} \;\; z \tag{2.27}$$

which is *not* of the type expected in Eq. (1.14) from renormalization.

2.6. Exact solution for ladders ($\alpha \neq 0$)

An exact solution to Eq. (2.23) for $\alpha \neq 0$ is found by Makeenko, Olesen, Semenoff (2006).

Let us consider the ansatz

$$\mathcal{G}\left(S,T;a,b\right) = \oint\limits_{C} \frac{d\omega}{2\pi i\omega} \left(\frac{S}{a}\right)^{\sqrt{\beta}\omega} \left(\frac{T}{b}\right)^{-\sqrt{\beta}\omega^{-1}} F\left(-\omega, \alpha\frac{a}{b}\right) F\left(\omega, \alpha\frac{S}{T}\right), \tag{2.28}$$

where C is a contour in the complex ω-plane. This ansatz is motivated by the integral representation of the Bessel function J_0 at $\alpha = 0$ ($\Longrightarrow F = 1$).

The substitution into Eq. (2.19) reduces it to the hypergeometric equation ($\xi = \alpha S/T$)

$$\xi(1+\xi)F''_{\xi\xi} + [1 + \sqrt{\beta}(\omega + \omega^{-1})](1+\xi)F'_{\xi} + \beta F = 0 \tag{2.29}$$

whose solution is given by hypergeometric functions. How to draw the contour C to satisfy the boundary conditions (2.21) is described in Appendix C.

A great simplification of the solution (2.28) occurs at $S = T$, $a = b$ and $\alpha = -1$:

$$\mathcal{G}_{\alpha=-1}(T,T;a,a) = \frac{1}{\sqrt{\beta\tau(\tau - 2\pi i)}} J_1\left(2\sqrt{\beta\tau(\tau-2\pi i)}\right) \tag{2.30}$$

with

$$\ln\frac{T}{a} = \tau\,, \qquad \ln\left(-\frac{T}{a}\right) = \tau - i\pi \tag{2.31}$$

and β given by Eq. (2.9).

In Appendix B this Bessel function is reproduced in the double-logarithmic approximation. It is similar to that obtained by Erickson, Semenoff, Zarembo (2000) for a circular Wilson loop. It is J_1 rather than I_1 because of Minkowski space.

Nothing good happens with the contribution of ladders to the cusp anomalous dimension. It is *not* of the form prescribed by the renormalizability (*cf.* Eq. (1.14)):

$$W\left(\varGamma_{\text{l.c.}}\right) \propto e^{-\frac{1}{4}f(\beta)\ln^2\frac{T}{a}}\,. \tag{2.32}$$

A mini conclusion of this fact is that diagrams with interaction have to contribute.

2.7. Two-loop ladder diagram

The contribution to the cusp anomalous dimension of the ladder diagram with two rungs depicted in Fig. 8 was calculated by Korchemsky, Radyushkin (1987).

The result is

$$\begin{aligned}\gamma_{\rm cusp}^{\rm (lad)} &= \frac{\lambda^2}{128\pi^4}\frac{(\cosh\theta-1)^2}{\sinh^2\theta}\int_0^\infty \frac{d\sigma}{\sigma}\ln\left(\frac{1+\sigma e^{\theta}}{1+\sigma e^{-\theta}}\right)\ln\left(\frac{\sigma+e^{\theta}}{\sigma+e^{-\theta}}\right)\\ &\to \frac{\lambda^2}{96\pi^4}\left(\theta^3+\frac{\pi^2}{2}\theta+\mathcal{O}(1)\right). \end{aligned} \tag{2.33}$$

The θ^3-term should be canceled by interaction! Therefore, not only ladder diagrams are essential to order λ^2.

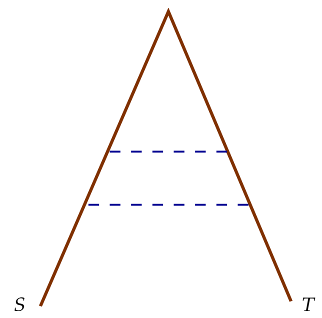

Fig. 8. Ladder diagram with two rungs.

Similar results hold for the light-cone Wilson loop, when

$$\mathcal{G}_{\rm l.c.}^{\rm ladd.} = 1-\frac{\beta}{2}\ln^2\frac{T}{\varepsilon}+\frac{\beta^2}{12}\ln^4\frac{T}{\varepsilon}-\frac{\beta^2\pi^2}{12}\ln^2\frac{T}{\varepsilon}\,. \tag{2.34}$$

The term $\ln^4\frac{T}{\varepsilon}$ is again to be canceled by diagrams with interaction.

2.8. Anomaly surface term

As was shown by Makeenko, Olesen, Semenoff (2006), the cancellation between the diagrams with the three-gluon vertex and the corrections to propagators (both are of the order λ^2) is *not* complete. These diagrams are depicted in Fig. 9.

The cancellation of the diagrams (b), (c) and (d) on the right-hand side is not complete as it is for a straight line or a circular loop. A nonvanishing surface term comes from integration by parts. It is represented by the

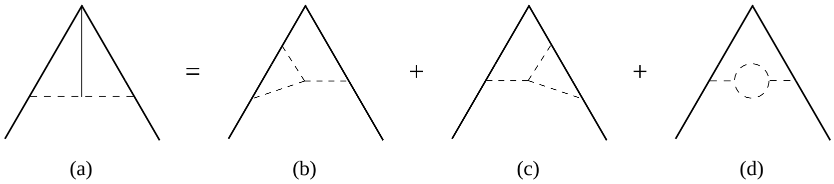

Fig. 9. Interaction diagrams of the order λ^2. The sum of the diagrams (b), (c) and (d) on the right-hand side is equal to the anomalous term represented by the diagram (a) on the left-hand side.

diagram (a) on the left-hand side. It gives the following contribution to the cusp anomalous dimension

$$\begin{aligned}\gamma_{\rm cusp}^{\rm anom} &= -\frac{\lambda^2}{16\pi^4}\frac{\cosh\theta-1}{\cosh\theta}\left(\int\limits_0^\theta+\int\limits_0^{\pi/2}\right)\frac{d\psi\,\psi}{1-\cosh^2\psi/\cosh^2\theta}\ln\frac{\cosh^2\theta}{\cosh^2\psi}\\ &\to -\frac{\lambda^2}{96\pi^4}\left(\theta^3+\pi^2\theta+\mathcal{O}(1)\right).\end{aligned}\tag{2.35}$$

The θ^3-terms are mutually canceled in the sum of the contributions of the ladder diagram (2.33) and the anomaly diagram (2.35). The remaining linear-in-θ term reproduces the known results

$$\gamma_{\rm cusp} = \frac{\theta}{2}\left(\frac{\lambda}{2\pi^2}-\frac{\lambda^2}{96\pi^2}\right)+\mathcal{O}(\theta^0)\tag{2.36}$$

for the two-loop cusp anomalous dimension.

Both the ladder contribution (2.33) and the anomaly contribution (2.35) simplify at the light cone. To demonstrate the exponentiation to the order λ^2, it is convenient to apply the so-called "non-Abelian exponentiation theorem" which states that

$$\ln W = \mathcal{G}^{(1)} + A^{(2)} - \mathcal{G}^{(2)}_{\rm crossed} + \mathcal{O}(\lambda^3)\,,\tag{2.37}$$

where $\mathcal{G}^{(2)}_{\rm crossed}$ denotes the ladder diagram with two *crossed* rungs, which is nonplanar and have to be added (and correspondingly subtracted) for the exponentiation of the diagram in Fig. 6(b) of the order λ.

We calculate the difference of the anomaly and crossed ladder diagram using the regularization via dimensional reduction to $d = 4-\epsilon$:

$$A^{(2)} - \mathcal{G}^{(2)}_{\rm crossed} = 2\beta^2\int\limits_a^S\frac{ds}{s^{1-\epsilon}}\int\limits_b^T\frac{dt}{t^{1-\epsilon}}\left[\frac{\pi^2}{6}-{\rm Li}_2\left(\frac{\alpha s}{\alpha s+t}\right)\right].\tag{2.38}$$

The integral in Eq. (2.38) is fast convergent when $s \to \infty$ or $t \to 0$ because $\mathrm{Li}_2(1) = \pi^2/6$. Alternatively, the second term (dilogarithm) can be omitted with the double-logarithmic accuracy for $\alpha s \ll t$. This justifies the exponentiation to the order λ^2 and reproduces the two-loop anomalous dimension because only the domain $\alpha s \lesssim t$ is essential both for $\alpha S \ll T$ and $\alpha S \gg T$.

2.9. Higher-order anomaly terms

A question arises as to whether the anomaly surface term of the order of β^2 is the only one (like an anomaly in QFT) or next order anomaly terms also appear. This question can be answered in the double logarithmic approximation.

Let us consider the sum of the ladder diagram with three rungs and the anomaly diagram of the order of λ^2 dressed by a ladder as is depicted in Fig. 10. It is easy to see that this sum does not provide the coefficient required for the exponentiation to the order λ^3, like in

$$W_{\mathrm{l.c.}}(\Gamma) = e^{-\frac{\beta}{2}\mathcal{T}^2}\,, \qquad \alpha S \gtrsim T\,, \tag{2.39}$$

which itself is a consequence of a dual conformal symmetry by Drummond, Korchemsky, Sokatchev (2008), Drummond, Henn, Korchemsky, Sokatchev (2008) and reviewed in the lectures by G. Korchemsky at this School.

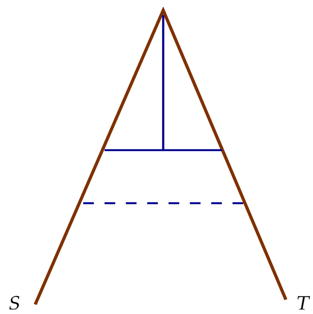

Fig. 10. Dressing of the anomaly diagram of the order λ^2 by a ladder.

However, to guarantee the exponentiation in the double logarithmic approximation to the order λ^3, it is enough to add a new anomaly diagram depicted in Fig. 11. It appears from a particular class of interaction diagrams of the order λ^3 after two integrations by parts.

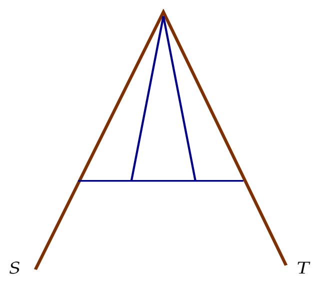

Fig. 11. New anomaly diagram of the order λ^3 which provides the exponentiation in the double logarithmic approximation.

2.10. Higher-order anomaly terms (continued)

The exponentiation to the order λ^3, described in the previous section, prompts to analyze anomaly diagrams of the type depicted in Fig. 12, *i.e.* of the type of a sliced pie.

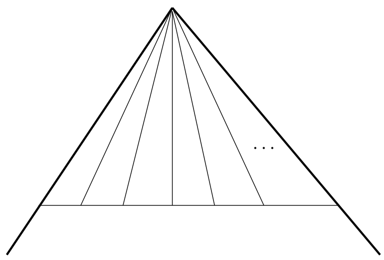

Fig. 12. Particular class of anomaly diagrams.

This class of diagrams can be exactly calculated recursively. Let us denote $x = -us$ and $y = vt$ with $y^2 = 0$ and $x^2 \neq 0$ to proceed recursively. We find for the n-loop (n-slice) diagram

$$\begin{aligned} P^{(n)}(x,y) \;=\; & 2^{n-1}(-1)^n \frac{\beta^n}{4(n-1)!} \left(\frac{4}{\epsilon}\right)^{n-1} \frac{\Gamma(1-\frac{n\epsilon}{2})}{\Gamma^n(1-\frac{\epsilon}{2})} \\ & \times u\cdot v \int\limits_0^S ds \int\limits_0^T dt \int\limits_0^1 d\tau_1 \cdots d\tau_{n-1} \frac{\prod_{k=1}^{n-1} \tau_k^{-k\epsilon/2}(1-\tau_k)^{-\epsilon/2}}{\left(x^2 - 2\prod_{k=1}^{n-1}\tau_k\, x\cdot y\right)^{1-n\epsilon/2}} \,. \end{aligned} \tag{2.40}$$

We have inserted a combinatorial factor of 2^{n-1} because the $n-1$ lines, that are trapped by the cusp, may come from both sides. Equation (2.40) is the exact result for the loop with 1 light-cone segment.

For the loop with 2 light-cone segments, we put $x^2 = 0$ after which the integral is expressed via Γ-functions:

$$P^{(n)} = (-1)^n \frac{\beta^n}{16(n!)^2} \left(\frac{4}{\epsilon}\right)^{2n} \frac{\Gamma(1-\frac{n\epsilon}{2})\Gamma(1+\frac{(n-1)\epsilon}{2})}{\Gamma(1-\frac{\epsilon}{2})} (2u \cdot vST)^{n\epsilon/2} \,. \tag{2.41}$$

It gives again the Bessel function J_0 in the double logarithmic approximation rather than the exponential (2.39).

In fact this illustrates why it is very difficult to obtain the exponential (2.39) in the framework of planar QFT, where the appearance of Bessel functions is instead quite natural and understandable from the relationship between connected planar and all planar diagrams. The exponential (2.39) is rather quite natural for Abelian theories when planar and nonplanar diagrams are both essential. Actually the role of the anomaly terms is simply to complete the Bessel function to an exponential.

A question immediately arises as to what is the equation which sums planar diagrams: ladders and anomalous to provide the exponentiation in the double logarithmic approximation? For this purpose we shall consider in the next section the cusped loop equation.

3. Cusped loop equation

In this section I consider the loop equation for cusped Wilson loops. I begin with a review of the modern formulation of the loop equation, describe its supersymmetric extension and a UV regularization. Then I concentrate on specific features of the loop equation for cusped loops and show how to extract the cusp anomalous dimension from the loop equation.

3.1. Loop equation in QCD

The Schwinger–Dyson equation of Yang–Mills theory

$$\nabla^{ab}_\mu F^b_{\mu\nu}(x) \overset{\text{w.s.}}{=} \hbar \frac{\delta}{\delta A^a_\nu(x)} \,, \tag{3.1}$$

when applied for Wilson loops, was translated by Makeenko, Migdal (1979) to the *loop equation* which is a closed equation as $N \to \infty$:

$$\partial^x_\mu \frac{\delta}{\delta\sigma_{\mu\nu}(x)} W(C) = \lambda \oint_C dy_\nu \, \delta^{(d)}(x-y) \, W(C_{yx}) \, W(C_{xy}) \,. \tag{3.2}$$

This original loop equation includes the operators of *path* and *area* derivatives, which are defined for functionals of Stokes type obeying the zig-zag symmetry. The product of two W's on the right-hand side is due to the large-N factorization.

The following vocabulary for translation from the ordinary space to loop space is in order.

Ordinary space		Loop space	
$\Phi[A]$	Phase factor	$\Phi(C)$	Loop functional
$F_{\mu\nu}(x)$	Field strength	$\dfrac{\delta}{\delta\sigma_{\mu\nu}(x)}$	Area derivative
∇^x_μ	Covariant derivative	∂^x_μ	Path derivative
$\nabla \wedge F = 0$	Bianchi identity		Stokes functionals
$-\nabla_\mu F_{\mu\nu} = \delta/\delta A_\nu$	Schwinger–Dyson equation		Loop equation

3.2. *Loop-space Laplace equation*

A very nice (and equivalent!) form of the loop equation can be obtained by one more contour integration over x:

$$\Delta W(C) = \lambda \oint_C dx_\mu \oint_C dy_\mu \, \delta^{(d)}(x-y)\, W(C_{yx})\, W(C_{xy})\,. \tag{3.3}$$

The operator Δ on the left-hand side of Eq. (3.3) is nothing but the loop-space Laplacian

$$\Delta \equiv \oint_C dx_\nu \, \partial^x_\mu \frac{\delta}{\delta\sigma_{\mu\nu}(x)} = \int_{\sigma_i}^{\sigma_f} d\sigma \int_{\sigma-0}^{\sigma+0} d\sigma' \frac{\delta}{\delta x_\mu(\sigma')} \frac{\delta}{\delta x_\mu(\sigma)} \tag{3.4}$$

which is a proper functional extension of a finite-dimensional Laplacian that respects continuity of the loop. As is seen from the right-hand side of Eq. (3.4), the loop-space Laplacian is defined for a much wider class of functionals than Stokes functionals. This will be important for a supersymmetric extension of the loop equation.

The loop-space Laplace equation (3.3) is associated with the second-order Schwinger–Dyson equation

$$\int d^d x \, \nabla_\mu F^a_{\mu\nu}(x) \frac{\delta}{\delta A^a_\nu(x)} \overset{\text{w.s.}}{=} \hbar \int d^d x \, d^d y \, \delta^{(d)}(x-y) \frac{\delta}{\delta A^a_\nu(y)} \frac{\delta}{\delta A^a_\nu(x)} \tag{3.5}$$

in the same sense as the original loop equation (3.2) is associated with Eq. (3.1). This fact was utilized by Halpern, Makeenko (1989) to construct a non-perturbative gauge-invariant regularization of Eq. (3.4) by substituting

$$\delta^{bc}\delta^{(d)}(x-y) \overset{\text{reg.}}{\Longrightarrow} \left\langle y \left| \left(e^{a^2\nabla^2/2}\right)^{bc} \right| x \right\rangle \,, \tag{3.6}$$

where a is a UV cutoff.

3.3. Smearing of loop-space Laplacian

A smearing of the loop-space Laplacian is needed to invert it, *i.e.* to produce a Green function.

The proper smearing procedure (which makes a second-order operator from the first order loop-space Laplacian) reads as

$$\begin{aligned} \Delta^{(G)} &= \int_0^1 d\sigma \int_0^1 d\sigma' \, G(\sigma,\sigma') \frac{\delta}{\delta x_\mu(\sigma')} \frac{\delta}{\delta x_\mu(\sigma)} \\ &= \int_0^1 d\sigma \fint_0^1 d\sigma' \, G(\sigma,\sigma') \frac{\delta}{\delta x_\mu(\sigma')} \frac{\delta}{\delta x_\mu(\sigma)} + \Delta \end{aligned} \tag{3.7}$$

with the parametric-invariant smearing function

$$G(\sigma_1,\sigma_2) = e^{-\left|\int_{\sigma_1}^{\sigma_2} d\sigma \sqrt{\dot{x}^2(\sigma)}\right|/\varepsilon} \qquad (\varepsilon \ll L = \text{length})\,. \tag{3.8}$$

Here ε has the meaning of a *stiffness* of the loop.

3.4. Green function of functional Laplacian

Loop-space Laplacian was inverted by Makeenko (1988) to produce a Green function which is useful for an iterative solution.

The functional Laplace equation

$$\Delta^{(G)} W[x] = J[x] \tag{3.9}$$

with the proper choice of boundary conditions can be solved for a given $J[x]$ to give

$$W[x] = 1 - \frac{1}{2} \int_0^\infty dA \left\{ \left\langle J[x+\sqrt{A}\xi] \right\rangle_\xi^{(G)} - \left\langle J[\sqrt{A}\xi] \right\rangle_\xi^{(G)} \right\} \,. \tag{3.10}$$

The average over the loops $\xi(\sigma)$ in Eq. (3.10) is given by the path integral

$$\langle F[\xi]\rangle_{\xi}^{(G)} = \frac{\int_{\xi(0)=\xi(1)} D\xi e^{-S} F[\xi]}{\int_{\xi(0)=\xi(1)} D\xi e^{-S}} \tag{3.11}$$

over closed trajectories with the local action

$$S = \frac{1}{4}\int_0^1 d\sigma \left\{ \frac{\varepsilon}{\sqrt{\dot{x}^2(\sigma)}}\,\dot{\xi}^2(\sigma) + \frac{\sqrt{\dot{x}^2(\sigma)}}{\varepsilon}\,\xi^2(\sigma)\right\}. \tag{3.12}$$

This extends the results of the French mathematician R. Gâteaux (early 1900's) for the functional Laplacian (obtained for the case of L_2 space of functions with an integrable square) to the case of loop space when loops are always continuous functions. It is immediately seen from the action (3.12) that the presence of the stiffness ε is crucial to have a Wiener-type measure in the path integral (3.11) and correspondingly continuous trajectories.

3.5. Iterative solution

In large-N Yang–Mills theory the regularized $J[x]$ is as above bilinear in W:

$$\begin{aligned} J^{(G)}[x] \;=\; & \lambda \int_0^1\int_0^1 d\sigma_1 d\sigma_2\,(1-G(\sigma_1-\sigma_2))\,\dot{x}^\mu(\sigma_1)\dot{x}^\mu(\sigma_2) \\ & \times \int_{r(0)=x(\sigma_1)}^{r(a^2)=x(\sigma_2)} \mathcal{D}r e^{-\frac{1}{2}\int_0^{a^2} d\tau\,\dot{r}^2(\tau)} \\ & \times W(C_{x(\sigma_1)x(\sigma_2)} r_{x(\sigma_2)x(\sigma_1)})\, W(C_{x(\sigma_2)x(\sigma_1)} r_{x(\sigma_1)x(\sigma_2)})\,. \end{aligned} \tag{3.13}$$

It can been shown that an iterative solution in λ starting from $W_0(C)=1$ recovers Yang–Mills perturbation theory. All that can be deduced from the general formula

$$\left\langle e^{\mathrm{i}\sqrt{A}\int d\sigma \dot{p}(\sigma)\xi(\sigma)}\right\rangle_{\xi}^{(G)} = e^{-A\int d\sigma\int d\sigma' \dot{p}(\sigma)G(\sigma-\sigma')\dot{p}(\sigma')/2}, \tag{3.14}$$

where $p^\mu(\sigma)$ ($p^\mu(0)=p^\mu(1)$) represents a momentum-space loop. In particular, the triple gluon vertex remarkably appears from doing an uncertainty $\varepsilon \times 1/\varepsilon$.

3.6. SYM loop equation

An extension of the loop equation (3.3) to $\mathcal{N}=4$ SYM was proposed by Drukker, Gross, Ooguri (1999). An equivalent equation was derived earlier by Fukuma, Kawai, Kitazawa, Tsuchiya (1998) in connection with the IIB matrix model.

The equation closes for general supersymmetric loops

$$\boldsymbol{C} = \{x_\mu(\sigma), Y_i(\sigma); \zeta(\sigma)\} \qquad \mu = 1, \dots, 4, \; i = 1, \dots, 6\,, \tag{3.15}$$

where $\zeta(\sigma)$ denotes the Grassmann odd component. An $\mathcal{N}=4$ supersymmetric extension of the loop-space Laplacian (3.4) is

$$\boldsymbol{\Delta} = \lim_{\eta\to 0} \int ds \int_{s-\eta}^{s+\eta} ds' \left(\frac{\delta^2}{\delta x^\mu(s')\delta x_\mu(s)} + \frac{\delta^2}{\delta Y^i(s')\delta Y_i(s)} + \frac{\delta^2}{\delta\zeta(s')\delta\bar{\zeta}(s)} \right). \tag{3.16}$$

To return to the SYM Wilson loops (1.16), we have to put $\dot{Y}^2 = \dot{x}^2$, $\zeta = 0$ after acting by $\boldsymbol{\Delta}$. We use the bold $\boldsymbol{C}$ for general loops (3.15) and normal C for SYM loops (1.25).

The resulting $\mathcal{N}=4$ SYM loop equation then reads

$$\begin{aligned} \boldsymbol{\Delta} \ln W(\boldsymbol{C})\Big|_{\boldsymbol{C}=C} &= \lambda \int d\sigma_1 \int d\sigma_2 \; (\dot{x}_\mu(\sigma_1)\dot{x}_\mu(\sigma_2) - |\dot{x}_\mu(\sigma_1)||\dot{x}_\mu(\sigma_2)|) \\ &\quad \times \delta^{(4)}(x_1 - x_2) \frac{W(C_{x_1x_2})W(C_{x_2x_1})}{W(C)}\,. \end{aligned} \tag{3.17}$$

For latter convenience we have applied $\boldsymbol{\Delta}$ to $\ln W(\boldsymbol{C})$ and used the fact that $\boldsymbol{\Delta}$ is a first-order operator (obeys the Leibnitz rule). The right-hand side is correspondingly divided by $W(C)$.

Probably a simpler version of $\mathcal{N}=4$ SYM loop equation exists which is written directly for SYM loops $W(C)$ along the line of the derivation of the loop equation for an Abelian scalar loop by Makeenko (1988). It is crucial for this approach that the loop-space Laplacian is well-defined for the functionals of the type (1.16) which do *not* obey the zig-zag symmetry because of the presence of $\sqrt{\dot{x}^2}$. But Eq. (3.17) will be enough for the purposes below.

3.7. Cusped loop equation

The loop equation for cusped Wilson loops, which we denote by $\mathit{\Gamma}$, can be obtained by substituting $C = \mathit{\Gamma}$ in Eq. (3.17). We then obtain the following cusped loop equation

$$\mathbf{\Delta} \ln W(\boldsymbol{C})\Big|_{\boldsymbol{C}=\Gamma} = \lambda \int d\sigma_1 \int d\sigma_2 \; (\dot{x}_\mu(\sigma_1)\dot{x}_\mu(\sigma_2) - |\dot{x}_\mu(\sigma_1)||\dot{x}_\mu(\sigma_2)|) \times \delta^{(4)}(x_1 - x_2) \frac{W(\Gamma_{x_1 x_2}) W(\Gamma_{x_2 x_1})}{W(\Gamma)} \,. \tag{3.18}$$

The cusped loop equation (3.18) has several remarkable properties. One of them is the following. The right-hand side of the usual Yang–Mills loop equation (3.3) is of the order of L/a^3, where a is a UV cutoff. For the $\mathcal{N} = 4$ SYM loop equation (3.17) this term is canceled by scalars so the right-hand side of Eq. (3.17) is $\sim (La)^{-1}$ for smooth loops. But it is easy to estimate that it is $\sim a^{-2}$ for cusped loops which is larger. Therefore, some interesting information about cusped Wilson loop can be extracted from the loop equation at the order $\sim a^{-2}$. As we shall now see, this is the cusp anomalous dimensions.

A crucial observation is the following relation that holds for cusped Wilson loops:

$$\Delta \ln W(C)\Big|_{C=\Gamma} = -\frac{d}{da^2} \ln W(\Gamma) + \mathcal{O}(a^{-1}) \,. \tag{3.19}$$

Here the differential operator on the right-hand side which is, in general, regularization-dependent is written for the Schwinger proper time regularization, like in Eq. (3.13). The relation (3.19) can be verified in perturbation theory for usual Yang–Mills and most probably extends to the SYM case.

Noting that the term of the order a^{-2} on the right-hand side of Eq. (3.19) gives the cusped anomalous dimension owing to Eq. (1.5), we find that the cusp anomalous dimension equals to the term of the order a^{-2} on the right-hand side of the (regularized) loop equation:

$$\frac{2}{a^2} \gamma_{\text{cusp}}(\theta, \lambda) + \mathcal{O}\left(a^{-1}\right) = \lambda \int d\sigma_1 \int d\sigma_2 (\dot{x}_\mu(\sigma_1)\dot{x}_\mu(\sigma_2) - |\dot{x}_\mu(\sigma_1)||\dot{x}_\mu(\sigma_2)|) \times \delta_a^{(4)}(x_1 - x_2) \frac{W(\Gamma_{x_1 x_2}) W(\Gamma_{x_2 x_1})}{W(\Gamma)} \,. \tag{3.20}$$

Here the right-hand side is to be regularized according to Eq. (3.13).

This very interesting fact was first observed to the order λ of perturbation theory by Drukker, Gross, Ooguri (1999) and verified to order λ^2 for arbitrary θ by Makeenko, Olesen, Semenoff (2006). The nontrivial function of θ thus reproduced to the order λ^2 is the sum of the contribution of the ladder diagram (2.33) and the anomaly diagram (2.35).

The contribution of the ladder diagram of the order of λ^2 straightforwardly comes iteratively by substituting the ladder diagram of the order of λ into the right-hand side of Eq. (3.20). A planar part is canceled between the numerator and the denominator on the right-hand side of Eq. (3.20) so what is left is analogous to the diagram with two crossed ladders (with the minus sign) as in Eq. (2.33). This is a well-know implementation of the "non-Abelian exponentiation theorem" in the loop equation.

Alternatively, the contribution of the anomaly diagram is reproduced in a very nontrivial way, when a gluon is attached to the regularizing path $r_{x_1x_2}$. While the length of this path is $\sim a$, *i.e.* very small, this smallness is compensated by a very large factor. The calculation is performed using an important formula of the loop dynamics derived by Makeenko, Migdal (1981):

$$\int\limits_{\substack{z(0)=x\\ z(\tau)=y}} \mathcal{D}z(t) e^{-\int_0^\tau dt\, \dot{z}^2(t)/2} \int\limits_x^y dz^\mu \delta^{(d)}(z-u) = \int\limits_0^\infty d\tau_1 \int\limits_0^\infty d\tau_2\, \delta\left(\tau-\tau_1-\tau_2\right)$$
$$\times \frac{1}{(2\pi\tau_1)^{d/2}} e^{-(x-u)^2/2\tau_1} \frac{\overleftrightarrow{\partial}}{\partial u_\mu} \frac{1}{(2\pi\tau_2)^{d/2}} e^{-(y-u)^2/2\tau_2}\,. \tag{3.21}$$

This formula in the usual Yang–Mills theory was used to reproduce the three gluon vertex. Now in $\mathcal{N}=4$ SYM it reproduces directly the anomaly diagram, rather than individual interaction diagrams.

An expectation is that the loop equation may be useful for analyzing next orders in λ and, in particular, to verify the exponentiated solution (2.39) in the double logarithmic approximation.

3.8. Some comments about large-N QCD

Some of the results described above for cusped Wilson loops in $\mathcal{N}=4$ SYM are applicable also to large-N QCD. Actually, nobody considered before specific features of the loop equation for cusped loops.

A first immediate consequence of the cusped loop equations is that $|\dot{x}|$ on the right-hand side (which comes from scalars) can be neglected near the light-cone, reproducing the same cusped loop equation as in QCD.

This may indicate that $\gamma_{\rm cusp}$ coincide in both cases while the difference is absorbed by the charge renormalization which is present in QCD and missing in $\mathcal{N}=4$ SYM. This may be understood because supersymmetry is broken by construction in the presence of a cusp and the larger the cusp the larger is the breaking. However, this assertion is in fact rather vague because the cusp anomalous dimension is regularization-dependent. But this indeed works to the order λ^2, if the regularization in both cases is via dimensional reduction. A comparison of recent explicit calculations of the anomalous dimensions of twist-two operators to the order λ^3 in QCD by Moch, Vermaseren, Vogt (2004) with those in SYM by Kotikov, Lipatov, Onishchenko, Velizhanin (2004) may be useful for this purpose.

4. Conclusions

I list below a (quite incomplete) set of conclusions from this paper:

- Cusped Wilson loops are convenient for studies of the anomalous dimensions;
- The minimal surface of an open string in $\mathrm{AdS}_5 \otimes S^5$ determines the cusp anomalous dimension at large λ via the AdS/CFT correspondence;
- Ladder diagrams themselves do not give a reasonable result for the cusp anomalous dimension, so that diagrams with interaction are essential;
- A cancellation of interaction diagram to the order λ^2 is not complete for $\mathcal{N} = 4$ SYM cusped Wilson loops and an anomaly surface term remains;
- Results in the double logarithmic approximation indicate that higher-order interaction diagrams are also essential for the exponentiation;
- The loop equation has specific features for cusped loops when its right-hand side reproduces the cusp anomalous dimension;
- There are indications that some of the results about the cusp anomalous dimension in $\mathcal{N} = 4$ SYM could persist for QCD;
- A challenging problem is to obtain $\sqrt{\lambda}$ for large λ in perturbation theory.

Appendix A

Minimal surface in $\mathrm{AdS}_5 \otimes S^5$

I briefly review in this Appendix the calculation of the cusp anomalous dimension at large λ which is based on the open-string/Wilson-loop correspondence described in Sect. 1.10. Only the leading order calculation by Kruczenski (2002), Makeenko (2003) in the supergravity approximation is considered.

Near cusp ansatz

We describe the AdS_5 space by the Poincaré coordinates

$$x^0 = t\,, \quad x^1 = x\,, \quad x^2 = x^3 = 0\,, \quad z \tag{A.1}$$

choosing the Π-shaped loop to be located in the $0,1$-plane. The associated AdS_3 metric is

$$ds^2 = R^2 \frac{dt^2 - dx^2 - dz^2}{z^2}\,. \tag{A.2}$$

We parametrize the string worldsheet by the coordinates $\tau = t$, $\sigma = x$ so the open-string action reads as

$$A = -\frac{R^2}{2\pi\alpha'} \int\limits_0^y dx \int\limits_x^\infty dt \frac{1}{z^2} \sqrt{1 + \left(\frac{\partial z}{\partial x}\right)^2 - \left(\frac{\partial z}{\partial t}\right)^2} \,. \tag{A.3}$$

It is to be minimized for the function $z(t, x)$.

Using scale and Lorentz invariance (at the worldsheet) the following ansatz was proposed by Drukker, Gross, Ooguri (1999) near the cusp to simplify the problem of minimizing the action (A.3):

$$z(t, x) = \sqrt{t^2 - x^2} \frac{1}{f(\theta)} \,, \qquad \theta = \operatorname{arctanh} \frac{x}{t} \,. \tag{A.4}$$

It works for the domain near the cusp depicted in Fig. 13. As we shall see shortly it is the domain which contributes to the cusp anomalous dimension at large θ and at the light cone.

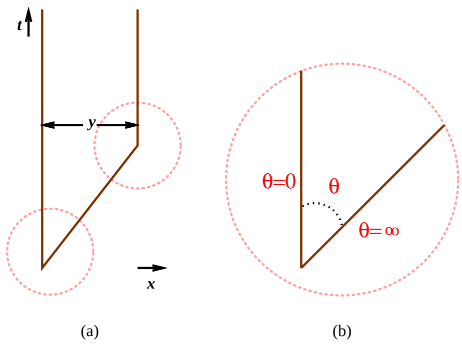

Fig. 13. Near cusp domains of the minimal surface which determines the cusp anomalous dimension. In part (b) one of the two domains is magnified.

The original two-dimensional variational problem is thus reduced to a one-dimensional Euler–Lagrange one.

Euler–Lagrange problem

We are led to minimize the one-dimensional action

$$A = -2\frac{R^2}{2\pi\alpha'} \int \frac{dx}{x} \int d\theta \sqrt{f^4 - f^2 + f'^2} \,, \tag{A.5}$$

where the factor of 2 is because the Π-shaped Wilson loop in Fig. 13(a) has two cusps.

The standard condition that $z = 0$ in the boundary is transformed into the boundary condition for $f(\theta)$: $f(0) = \infty$ and an arbitrary value of $f(\infty)$ because $\sqrt{t^2 - x^2} \to 0$ as $\theta \to \infty$. Also, $f = 0$ is the horizon and $f = 1$ is the AdS light cone given by $z^2 = t^2 - x^2$.

To minimize the action (A.5), we solve the following Euler–Lagrange equation

$$f''V = f'^2V' + \frac{1}{2}V'V\,, \qquad V = f^4 - f^2 \tag{A.6}$$

with the described boundary conditions.

Solution for $f(\theta)$

The equation (A.6) can be easily integrated utilizing the conserved "energy"

$$E = \frac{V}{\sqrt{f'^2 + V}} \qquad \Longrightarrow \qquad f' = -\sqrt{\frac{V^2}{E^2} - V}\,. \tag{A.7}$$

It is seen from these formulas that $\theta_{\max}$ is finite unless $E^2 = -1/4 < 0$ (an instanton-like solution).

An exact analytic solution to Eq. (A.7) is

$$\theta = \sqrt{2}\,\mathrm{arctanh}\sqrt{2(1-f^2)} - \mathrm{arctanh}\sqrt{1-f^2} - \frac{\mathrm{i}\pi}{2}\left(\sqrt{2}-1\right). \tag{A.8}$$

It obeys the boundary condition $\theta = 0$ at $f = \infty$ and $\theta \to \infty$ approaching the light cone as $f \to f_{\min} = 1/\sqrt{2}$.

Only a part of the surface near the light cone described by the equation

$$z = \frac{\sqrt{t^2 - x^2}}{f_{\min}} = \sqrt{2(t^2 - x^2)} \tag{A.9}$$

will be essential for the cusp anomalous dimension. It is the same (space-like) minimal surface as found by Kruczenski (2002) for space-like Wilson loops, when it was always real.

Cusp anomalous dimension

Substituting the solution (A.8) into the action (A.5), we find that the essential domain of integration is when

$$f \to f_{\min} = \frac{1}{\sqrt{2}} + \sqrt{2}e^{-\sqrt{2}\theta_{\max}}\,, \qquad \theta_{\max} = \ln\frac{2\sqrt{2}x}{a} \tag{A.10}$$

and $\theta \to \theta_{\max}$. We get for the divergent part of the minimal area

$$
\begin{aligned}
A_{\min} &= \frac{R^2}{\pi\alpha'} \int\limits_a^y \frac{dx}{x} \int\limits_0^{\theta_{\max}} d\theta \sqrt{f_{\min}^4 - f_{\min}^2} \\
&= i\frac{R^2}{\pi\alpha'} \int\limits_a^y \frac{dx}{x}\frac{\theta_{\max}}{2} = i\frac{R^2}{4\pi\alpha'}\ln^2\frac{y}{a}\,.
\end{aligned}
\tag{A.11}
$$

From the open-string/Wilson-loop correspondence, described in Sect. 1.10, we obtain

$$
W_{\mathrm{SYM}}(\Pi) = e^{2\mathrm{i}A_{\min}} \qquad \text{with} \quad \sqrt{\lambda} = \frac{R^2}{\alpha'}. \tag{A.12}
$$

Comparing with Eq. (1.14) we find

$$
f(\lambda) = \frac{\sqrt{\lambda}}{\pi}\,, \qquad \text{large } \lambda \tag{A.13}
$$

which reproduces the result by Gubser, Klebanov, Polyakov (2002) quoted in Sect. 1.9. It is obtained for open string in the supergravity approximation while the original calculation dealt with closed string in the plane wave limit.

The asymptotic behavior (A.13) of the cusp anomalous dimension at large λ has been remarkably reproduced from the spin-chain equation of Beisert, Eden, Staudacher (2007) first numerically by Benna, Benvenuti, Klebanov, Scardicchio (2007) and then analytically by Kotikov, Lipatov (2007), Basso, Korchemsky, Kotanski (2008). The later authors constructed a systematic expansion of the cusp anomalous dimension in $1/\sqrt{\lambda}$, reproducing also the $\mathcal{O}(1)$ correction by Frolov, Tseytlin (2002) obtained from closed stings. The next order in $1/\sqrt{\lambda}$ also agrees with the recent superstring calculations by Roiban and Tseytlin (2007), (2008).

Appendix B

Double-logarithmic accuracy

I describe in this appendix how the double logarithmic accuracy works for lightcone Wilson loops to the leading order, confirming in particular previously obtained results.

Double logarithms at the light cone

Let us consider the 1 light-cone limit with $\beta \ll 1$ while

$$
\mathcal{T} = \ln\frac{T}{\alpha a}\,, \qquad \Sigma = \ln\frac{S}{a} \tag{B.1}
$$

are both large for the double Logs to be of order 1. We assume $\alpha > 0$ (for $\alpha < 0$ it should be substituted by $|\alpha|$).

The double Logs appear in the ladder equation (2.17) from the domain of integration $t \gg \alpha s$, so we rewrite it with DLA as

$$\mathcal{G}\left(S,T;a,b\leq\alpha a\right)=1-\beta\int\limits_{a}^{\min\{S,T/\alpha\}}\frac{ds}{s}\int\limits_{\max\{\alpha s,b\}}^{T}\frac{dt}{t}\,\mathcal{G}\left(s,t;a,b\leq\alpha a\right). \tag{B.2}$$

We solve it first for $\mathcal{G}\left(S,T\geq\alpha S;a,b\right)$, which then determines $\mathcal{G}\left(S,T\leq\alpha S;a,b\right)$ in DLA.

Leading-order solution

An exact solution to Eq. (B.2) for $b \leq \alpha a$ is given by the sum of two Bessel functions

$$\mathcal{G}\left(S,T\geq\alpha S;a,b\leq\alpha a\right)=J_0\left(2\sqrt{\beta\Sigma\mathcal{T}}\right)+\frac{\Sigma}{\mathcal{T}}J_2\left(2\sqrt{\beta\Sigma\mathcal{T}}\right). \tag{B.3}$$

The first term on the RHS of Eq. (B.3) is familiar from the $\alpha = 0$ solution. But now the solution is for any α with DLA.

The solution (B.3) obeys the boundary condition $\mathcal{G}(a,T;a,b)=1$. The second one, $\mathcal{G}(S,b;a,b)=1$, cannot be verified because $T\geq\alpha S$. Instead (B.3) obeys

$$\frac{\partial}{\partial S}\,\mathcal{G}(S,T\geq\alpha S;a,b)\Big|_{S=T/\alpha}=0 \tag{B.4}$$

at the boundary $S = T/\alpha$, which can be deduced from Eq. (B.2).

Substituting $S = T/\alpha$ we have from Eq. (B.3)

$$\mathcal{G}\left(T,T;a,b\leq\alpha a\right)=\frac{J_1\left(2\sqrt{\beta}\mathcal{T}\right)}{\sqrt{\beta}\mathcal{T}} \tag{B.5}$$

which is the same Bessel function as in Makeenko, Olesen, Semenoff (2006).

Finally, substituting Eq. (B.3) into Eq. (B.2), we get

$$\mathcal{G}\left(S\geq T/\alpha,T;a,b\leq\alpha a\right)=\frac{J_1\left(2\sqrt{\beta}\mathcal{T}\right)}{\sqrt{\beta}\mathcal{T}} \tag{B.6}$$

which does not depend on Σ with DLA. We can set $S = \infty$ in Eq. (B.6).

Appendix C

Exact sum of lightcone ladders

I describe in this appendix now to draw the contour in the complex ω-plane for the solution (2.28) with F obeying Eq. (2.29) to satisfy the boundary condition (2.21) and correspondingly to be a solution for the sum of the lightcone ladder diagrams.

The exact solution

The ansatz (2.28) with F obeying Eq. (2.29) will satisfy the boundary condition (2.21) if the integrand has no poles in the complex ω-plane. Then the contour of the integration over ω can be arbitrarily deformed.

The following linear combination of solutions of the hypergeometric equation (2.29) solves the problem as was shown by Makeenko, Olesen, Semenoff (2006):

$$
\begin{aligned}
G(S,T;a,b) &= \oint\limits_{C^r} \frac{d\omega}{2\pi i\omega}\, {}_2F_1\left(-\sqrt{\beta}\omega, -\sqrt{\beta}\omega^{-1}; 1-\sqrt{\beta}(\omega+\omega^{-1}); -\alpha\frac{a}{b}\right) \\
&\times \left(\frac{S}{a}\right)^{\sqrt{\beta}\omega} \left(\frac{T}{b}\right)^{-\sqrt{\beta}\omega^{-1}} {}_2F_1\left(\sqrt{\beta}\omega, \sqrt{\beta}\omega^{-1}; 1+\sqrt{\beta}(\omega+\omega^{-1}); -\alpha\frac{S}{T}\right) \\
&+ \int\limits_{|n_{\min}-0} \frac{ds}{2\pi i} \frac{\Gamma(-s)}{\Gamma(s)} \frac{1}{\sqrt{\beta}(\omega_+^{\mathrm{R}}-\omega_-^{\mathrm{R}})} \frac{\Gamma(\sqrt{\beta}\omega_+^{\mathrm{R}})\Gamma(1+\sqrt{\beta}\omega_+^{\mathrm{R}})}{\Gamma(\sqrt{\beta}\omega_+^{\mathrm{L}})\Gamma(1+\sqrt{\beta}\omega_+^{\mathrm{L}})} \\
&\times \left[\left(\frac{\alpha S}{b}\right)^{\sqrt{\beta}\omega_+^{\mathrm{R}}} \left(\frac{T}{\alpha a}\right)^{-\sqrt{\beta}\omega_-^{\mathrm{R}}} + \left(\frac{\alpha S}{b}\right)^{\sqrt{\beta}\omega_-^{\mathrm{R}}} \left(\frac{T}{\alpha a}\right)^{-\sqrt{\beta}\omega_+^{\mathrm{R}}}\right] \\
&\times {}_2F_1\left(\sqrt{\beta}\omega_+^{\mathrm{R}}, \sqrt{\beta}\omega_-^{\mathrm{R}}; s+1; -\alpha\frac{a}{b}\right) {}_2F_1\left(\sqrt{\beta}\omega_+^{\mathrm{R}}, \sqrt{\beta}\omega_-^{\mathrm{R}}; s+1; -\alpha\frac{S}{T}\right)
\end{aligned}
\tag{C.1}
$$

with

$$
\omega_\pm^{\mathrm{R}} = \frac{s}{2\sqrt{\beta}} \pm \sqrt{\frac{s^2}{4\beta}-1} \qquad \omega_\pm^{\mathrm{L}} = -\omega_\mp^{\mathrm{R}} = -\frac{s}{2\sqrt{\beta}} \pm \sqrt{\frac{s^2}{4\beta}-1}\,. \tag{C.2}
$$

The contour C^r in the first term runs over a circle of arbitrary radius r ($|\omega| = r$). The second contour integral runs parallel to imaginary axis along

$$
s = n_{\min} - 0 + ip \qquad (-\infty < p < +\infty)\,, \tag{C.3}
$$

where

$$n_{\min} = \left[\sqrt{\beta}(r + 1/r)\right] + 1 \tag{C.4}$$

and $[\cdots]$ denotes the integer part.

Cancellation of poles

The integrand in the first term on the right-hand side of Eq. (C.1) has poles at

$$\omega = \omega_{\pm}^{\mathrm{R}}(n) = \frac{n}{2\sqrt{\beta}} \pm \sqrt{\frac{n^2}{4\beta} - 1}\,, \qquad \omega = \omega_{\pm}^{\mathrm{L}}(n) = -\frac{n}{2\sqrt{\beta}} \pm \sqrt{\frac{n^2}{4\beta} - 1} \tag{C.5}$$

as the hypergeometric functions have. These poles are depicted in Fig. 14.

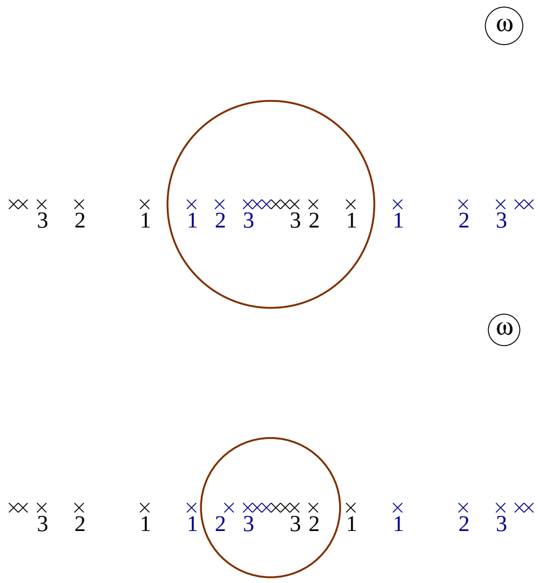

Fig. 14. Location of poles of the integrand in the first term in Eq. (C.1) for $\beta < \frac{1}{4}$, $r = 1$ (above) and $\beta < \frac{1}{4}$, $r < 1$ (below). The circle represents the contour of integration C^r.

The poles of the integrand in the first term are canceled by the poles at $s = n$ of the integrand in the second term, so the contour of integration can be arbitrarily deformed. This is guaranteed by the value of $n_{\min}$, given by Eq. (C.4), which changes accordingly with r to provide the cancellation of the poles of the first term, that are located inside C^r, by those of the second term, that are located to the right on $n_{\min}$.

The boundary conditions (2.21) are satisfied by the solution (C.1): we choose the integration contour in the first term to be a circle of the radius which is either small for $T = b$ or large for $S = a$. Then the residue at the pole at $\omega = 0$ or $\omega = \infty$ equals 1 which proves that the boundary conditions is satisfied.

For $S = T$, $a = b$ and $\alpha = -1$ the solution (C.1) simplifies to the Bessel function (2.30).

REFERENCES

Alday L.F., Maldacena J., *J. High Energy Phys.* **0706**, 064 (2007) [`0705.0303 [hep-th]`].

Alday L.F., Maldacena J., *J. High Energy Phys.* **0711**, 019 (2007) [`0708.0672 [hep-th]`].

Alday L.F., Maldacena J., *J. High Energy Phys.* **0711**, 068 (2007) [`0710.1060 [hep-th]`].

Alday L.F, Roiban R., *Acta Phys. Pol. B*, **39**, 2979 (2008), these proceedings.

Basso B., Korchemsky G.P., Kotanski J., *Phys. Rev. Lett.* **100**, 091601 (2008) [`0708.3933 [hep-th]`].

Beisert N., Eden B., Staudacher M., *J. Stat. Mech.* **0701**, P021 (2007) [`hep-th/0610251`].

Benna M.K., Benvenuti S., Klebanov I.R., Scardicchio A., *Phys. Rev. Lett.* **98**, 131603 (2007) [`hep-th/0611135`].

Berenstein D., Corrado R., Fischler W., Maldacena J., *Phys. Rev.* **D59**, 105023 (1999) [`hep-th/9809188`].

Bern Z., Dixon L.J., Smirnov V.A., *Phys. Rev.* **D72**, 085001 (2005) [`hep-th/0505205`].

Bern Z., Czakon M., Dixon L.J., Kosower D.A., Smirnov V.A., *Phys. Rev.* **D75**, 085010 (2007) [`hep-th/0610248`].

Brandt R.A., Neri F., Sato M., *Phys. Rev.* **D24**, 879 (1981).

Brodsky S.J., Frishman Y., Lepage G.P., Sachrajda C.T., *Phys. Lett.* **B91**, 239 (1980).

Dotsenko V.S., Vergeles S.N., *Nucl. Phys.* **B169**, 527 (1980).

Drukker N., Gross D.J., *J. Math. Phys.* **42**, 2896 (2001) [`hep-th/0010274`].

Drukker N., Gross D.J., Ooguri H., *Phys. Rev.* **D60**, 125006 (1999) [`hep-th/9904191`].

Drummond J.M., Henn J., Korchemsky G.P., Sokatchev E., *Nucl. Phys.* **B795**, 52 (2008) [`0709.2368 [hep-th]`].

Drummond J.M., Henn J., Korchemsky G.P., Sokatchev E., `0807.1095 [hep-th]`.

Drummond J.M., Korchemsky G.P., Sokatchev E., *Nucl. Phys.* **B795**, 385 (2008) [`0707.0243 [hep-th]`].

Eden B., Staudacher M., *J. Stat. Mech.* **0611**, P014 (2006) [hep-th/0603157].
Erickson J.K., Semenoff G.W., Szabo R.J., Zarembo K., *Phys. Rev.* **D61**, 105006 (2000) [hep-th/9911088].
Erickson J.K., Semenoff G.W., Zarembo K., *Nucl. Phys.* **B582**, 155 (2000) [hep-th/0003055].
Fukuma M., Kawai H., Kitazawa Y., Tsuchiya A., *Nucl. Phys.* **B510**, 158 (1998) [hep-th/9705128].
Frolov S., Tseytlin A.A., *J. High Energy Phys.* **0206**, 007 (2002) [hep-th/0204226].
Halpern M.B., Makeenko Y.M., *Phys. Lett.* **B218**, 230 (1989).
Gervais J.L., Neveu A., *Nucl. Phys.* **B163**, 189 (1980).
Gross D.J., Wilczek F., *Phys. Rev.* **D8**, 3633 (1973).
Gubser S.S., Klebanov I.R., Polyakov A.M., *Nucl. Phys.* **B636**, 99 (2002) [hep-th/0204051].
Korchemsky G.P., Marchesini G., *Nucl. Phys.* **B406**, 225 (1993).
Korchemsky G.P., Radyushkin A.V., *Nucl. Phys.* **B283**, 342 (1987).
Kotikov A.V., Lipatov L.N., *Nucl. Phys.* **B769**, 217 (2007) [hep-th/0611204].
Kotikov A.V., Lipatov L.N., Onishchenko A.I., Velizhanin V.N., *Phys. Lett.* **B595**, 521 (2004), Erratum: *Phys. Lett.* **B632**, 754 (2006) [hep-th/0404092].
Kruczenski M., *J. High Energy Phys.* **0212**, 024 (2002) [hep-th/0210115].
Maldacena J., *Phys. Rev. Lett.* **80**, 4859 (1998) [hep-th/9803002].
Makeenko Y.M., *Sov. J. Nucl. Phys.* **33**, 440 (1981).
Makeenko Y.M., *Phys. Lett.* **B212**, 221 (1988).
Makeenko Y., *Methods of Contemporary Gauge Theory*, Cambridge Univ. Press, 2002.
Makeenko Y., *J. High Energy Phys.* **0301**, 007 (2003) [hep-th/0210256].
Makeenko Y.M., Migdal A.A., *Phys. Lett.* **B88**, 135 (1979).
Makeenko Y.M., Migdal A.A., *Nucl. Phys.* **B188**, 269 (1981).
Makeenko Y., Olesen P., Semenoff G.W., *Nucl. Phys.* **B748**, 170 (2006) [hep-th/0602100].
Moch S., Vermaseren J.A.M., Vogt A., *Nucl. Phys.* **B688**, 101 (2004) [hep-ph/0403192].
Ohrndorf T., *Nucl. Phys.* **B198**, 26 (1982).
Polyakov A.M., *Nucl. Phys.* **B164**, 171 (1980).
Rey S.-J., Yee J., *Eur. Phys. J.* **C22**, 379 (2001) [hep-th/9803001].
Roiban R., Tseytlin A.A., *J. High Energy Phys.* **0711**, 016 (2007) [0709.0681 [hep-th]].
Roiban R., Tseytlin A.A., *Phys. Rev.* **D77**, 066006 (2008) [0712.2479 [hep-th]].
Semenoff G.W., Zarembo K., *Nucl. Phys. Proc. Suppl.* **108**, 106 (2002) [hep-th/0202156].
Staudacher M., *J. High Energy Phys.* **0505**, 054 (2005) [hep-th/0412188].
Wilson K.G., *Phys. Rev.* **D10**, 2445 (1974).